3. RESULTS

3.1. Microscopical Analysis of Murine Peyer's Patches and M Cells

To determine whether electron microscopy was a suitable method of analysis, Peyer's patches were excised from non-infected mice and processed for both transmission and scanning electron microscopy (TEM and SEM, respectively). Using TEM, it could be seen (Fig. 3.1A) that M cells are easily identifiable within the FAE. Due to the very small size of the sections (thickness and width) a good overview of a dome area was difficult to establish. So SEM was also performed (Fig. 3.1B) yielding an extremely good overview. The draw back of SEM is that only surface structures are visible, so both TEM and SEM were used in conjunction to obtain accurate and representative microscopical results. Segmented filamentous bacteria were also commonly seen colonising Peyer's patches (Fig. 3.2), but less commonly observed on villi, confirming similar findings of others (Klaasen et al, 1992).

Confocal Laser Scanning Microscopy (CLSM) was also performed on murine

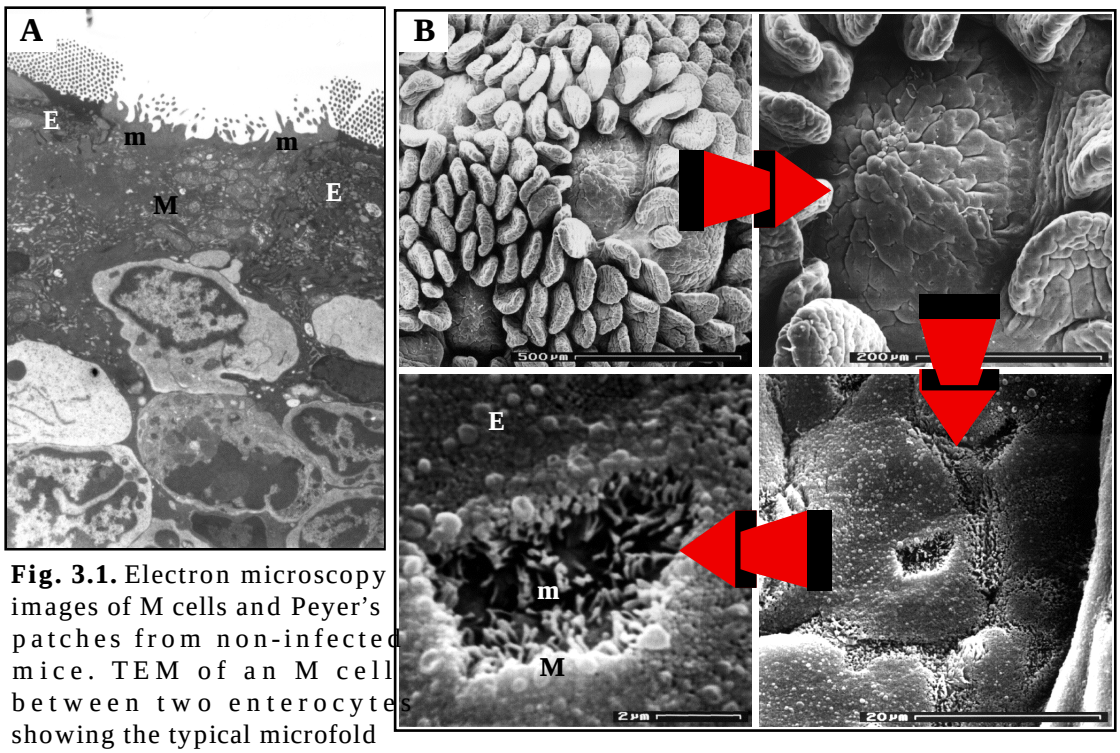

Fig. 3.1. Electron microscopy images of M cells and Peyer's patches from non-infected mice. TEM of an M cell between two enterocytes showing the typical microfold apical membrane morphology (A). SEM showing the surface structure of a Peyer's patch at different magnifications (B)- from top left, clockwise: Peyer's patch as seen from the lumen exhibiting multiple dome areas; a single dome area; enterocytes and M cells of a dome area; an M cell. M=M cell, E=enterocyte, m=microfolds.

Peyer's patches as this gave an extremely good overview of the tissue (Fig. 3.3) and allowed extra- and intracellular bacteria to be visualised. CLSM has a much lower resolution than TEM and SEM, but there is a specific marker for murine M cells, namely the lectin from *Ulex europaeus*-1 (UEA-1) which binds to fucose residues expressed on the apical cell surface of M cells. When used together, these results demonstrate the ease by which Peyer's patches can be examined using microscopical methods, and also reveal the

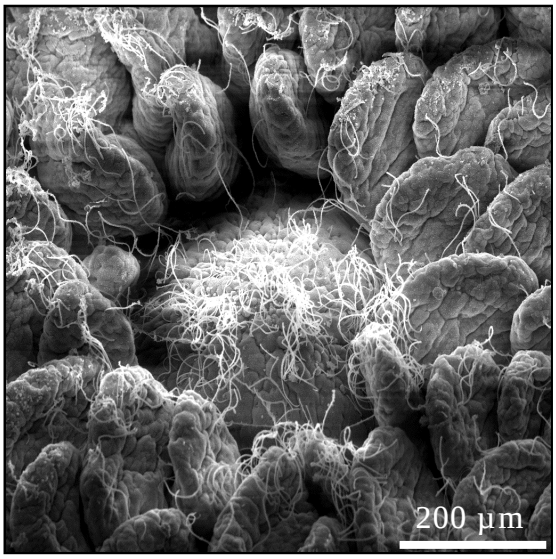

Fig. 3.2. Dome area showing segmented filamentous bacteria, commonly found as part of the normal flora in rodents.

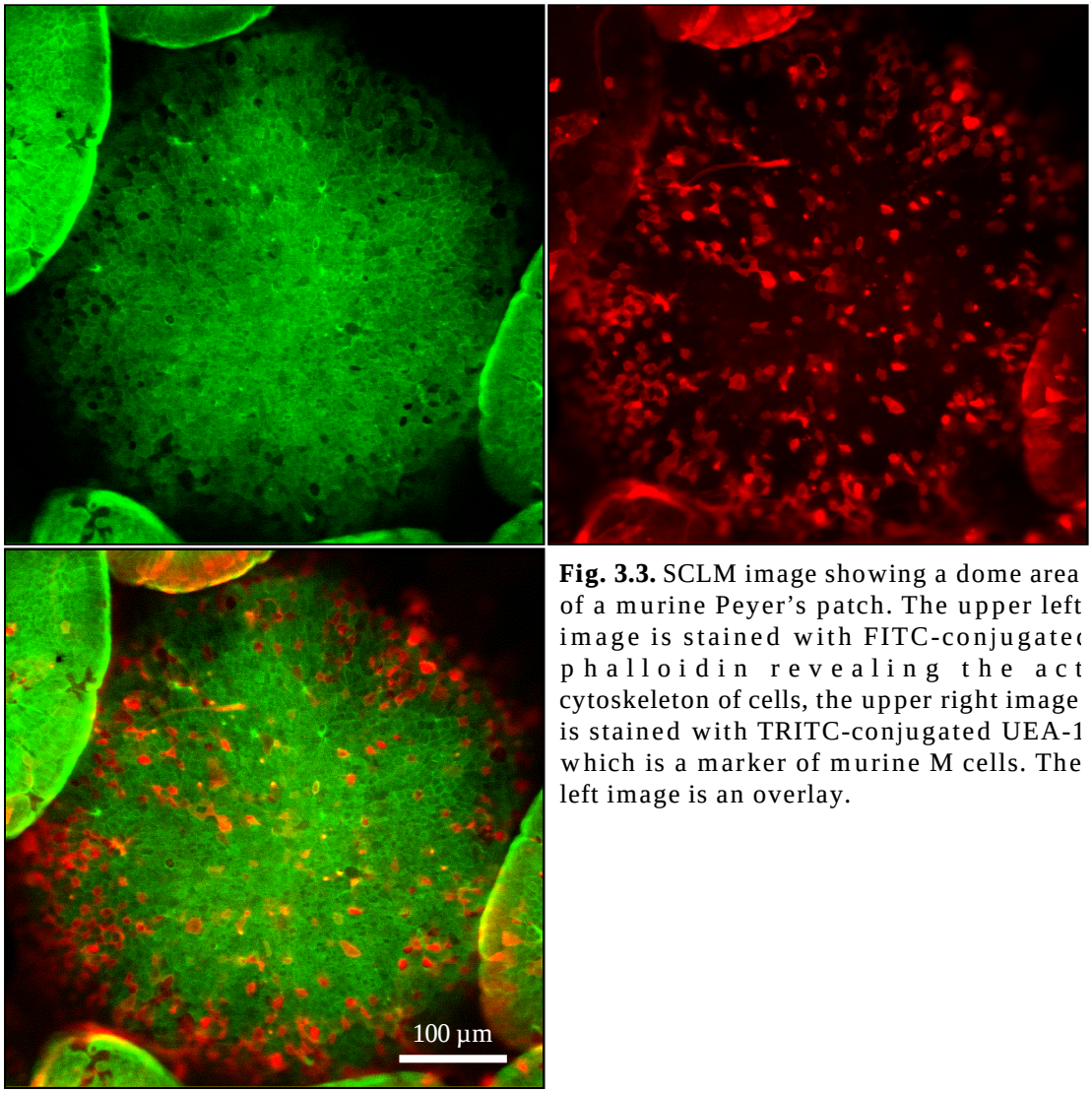

Fig. 3.3. SCLM image showing a dome area of a murine Peyer's patch. The upper left image is stained with FITC-conjugated phalloidin revealing the act cytoskeleton of cells, the upper right image is stained with TRITC-conjugated UEA-1 which is a marker of murine M cells. The left image is an overlay.

limitations of each method. However, used in conjunction with one another accurate results may be easily obtained.

3.2. SlyA of *S. typhimurium*

It has already been shown that inactivation of the *slyA* gene leads to marked attenuation of *S. typhimurium* in macrophage survival assays and in the mouse model (Libby et al, 1994). It was therefore undertaken to further characterise the effect of SlyA on virulence in the mouse model, and to go some way to identifying the biological function of SlyA.

3.2.1. Production of SlyA by *S. typhimurium* 14028s and Isogenic Derivatives of this Strain Affected in *slyA*

The expression of SlyA in *S. typhimurium* 14028s (WT), two *slyA* plasmid insertion mutants of *S. typhimurium* 14028s (SLYAI and SLYAII), and *S. typhimurium* 14028s / pAL102 (SLYA++), carrying multiple copies of *slyA*, was analysed by immunoblotting of whole cell proteins from logarithmic and stationary phase bacteria using a polyclonal anti-SlyA antiserum (Ludwig et al, 1995). As shown in Fig. 3.4, the WT strain carrying a single chromosomal copy of *slyA* produced small amounts of SlyA, only detectable in the stationary phase. *S. typhimurium* / pAL102 expressed, in both growth phases, considerably more SlyA protein than the WT strain. The *slyA* mutants, SLYAI and SLYAII, on the

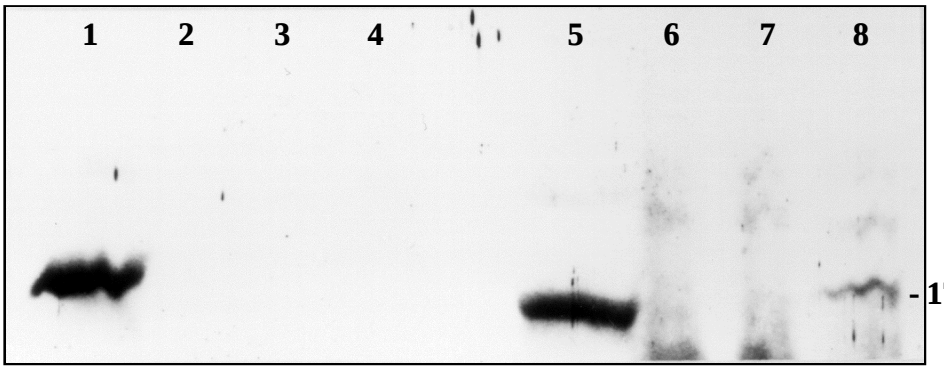

Fig. 3.4. Western blot analysis of *S. typhimurium* 14028s / pAL102 (lanes 1 and 5), SLYAI (lanes 2 and 6), SLYAII (lanes 3 and 7) and *S. typhimurium* 14028s (lanes 4 and 8). Lanes 1-4 are from logarithmic phase bacteria, and lanes 5-8 are from stationary phase bacteria.

other hand, synthesised no detectable amounts of SlyA during the logarithmic or stationary phase.

This confirmed the successful inactivation of the *slyA* gene in the two mutant strains SLYAI and SLYAII, and that strain SLYA++ also, successfully, over produced the SlyA protein.

3.2.2. Kinetic of SlyA Expression Using Western Blot Analysis

Due to the interesting observation that SlyA is only expressed in detectable amounts in the stationary phase of growth, the exact point in the growth phase that SlyA is expressed was determined under laboratory conditions. To this end, equivalent numbers of bacteria were taken at different time points from a freshly inoculated WT *S. typhimurium* LB broth culture, whole cell proteins isolated, and analysed on an SDS-PAGE gel. After blotting onto a nitrocellulose filter, the proteins were probed with an anti-SlyA antibody, as described above. It was seen that SlyA was only detectable in the late log growth phase of *S. typhimurium* WT (see Fig. 3.5).

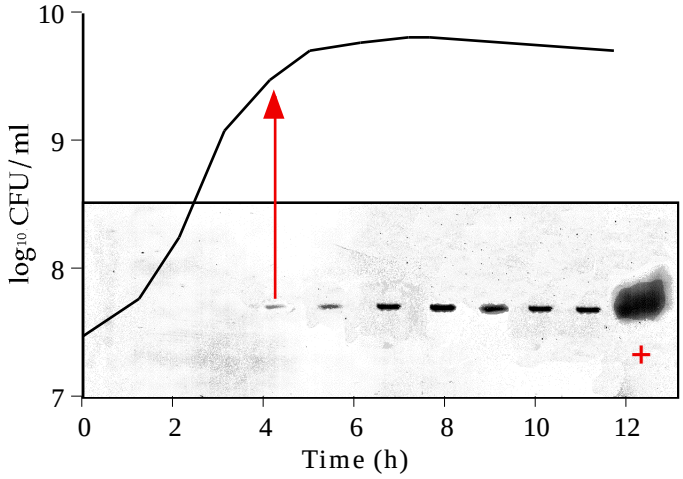

Fig. 3.5. Kinetic of SlyA production demonstrating detectable amounts of SlyA only in the late logarithmic phase of growth, and thereafter. The spot indicated with + is the positive control- proteins isolated from *S. typhimurium*/pAL102. Proteins were analysed using Western blot techniques with an anti-SlyA antibody as probe.

3.2.3. Two Dimensional Electrophoretic Gel Analysis of Proteins Affected in *slyA*

Given the recently published data indicating SlyA to be a regulator (Dehoux and Cossart, 1995, Ludwig et al, 1995 and Oscarsson et al, 1996), protein expression

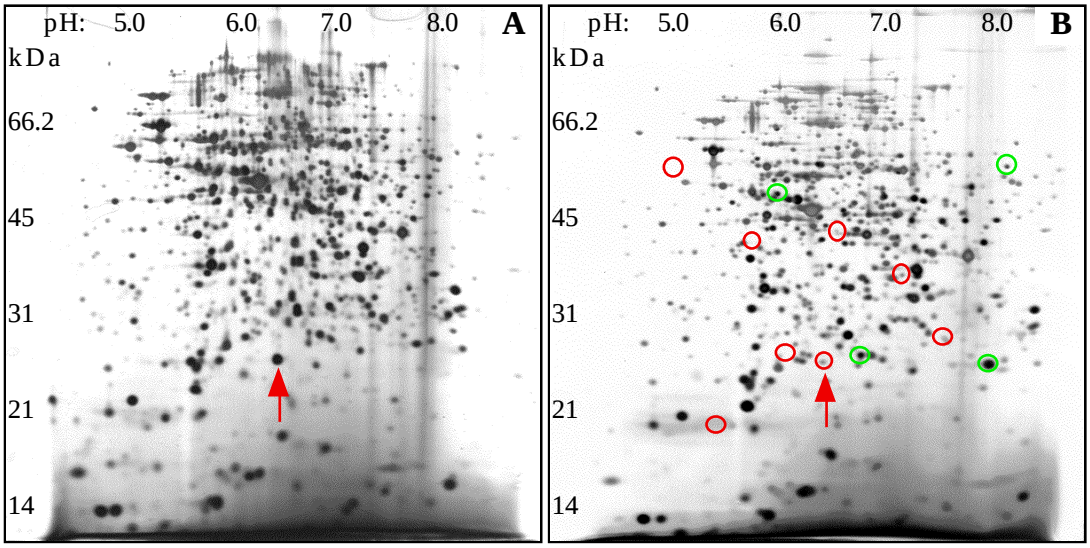

Fig. 3.6. Two-dimensional gel electrophoresis of whole cell proteins of WT *S typhimurium* (**A**) and SLYAII (**B**), showing some of the more noticeable differences. Green circles mark proteins consistently up-regulated in the SLYAII strain and red circles mark down-regulated proteins in SLYAII. The red arrow represents the position of a SodB-homologue. Gels courtesy of Isabel Lößner.

patterns of the wild type *S. typhimurium* strain, and mutant strain SLYAII, were analysed using two dimensional (2-D) gel electrophoresis of whole cell preparations, ie cytoplasmic, periplasmic and membrane proteins, from stationary phase (over night) cultures. Proteins from each strain were isolated on at least three separate occasions and analysed using 2-D gel electrophoresis at least three separate times. The proteins that were consistently in smaller or greater amounts are marked in Fig. 3.6B.

As shown in Fig. 3.6 numerous spots can be observed that were either additional or absent in the SLYAI and SLYAII strains, when compared to the isogenic wild type strain, indicating a global regulatory function for SlyA.

Analysis of the N-terminal amino acid sequences of some of these spots has been performed (reported in Lößner, 1998). The most interesting finding regarding this work is that one of the protein spots bears high homology to SodB of *Escherichia coli* (marked with arrow in Fig. 3.6). This will be discussed later in this work.

3.2.4. Colonisation and Invasion of the Small Intestine by the *S. typhimurium* Strains

To determine whether SlyA has any bearing on the proficiency of *S. typhimurium* to colonise the small intestine or invade Peyer's patches, four

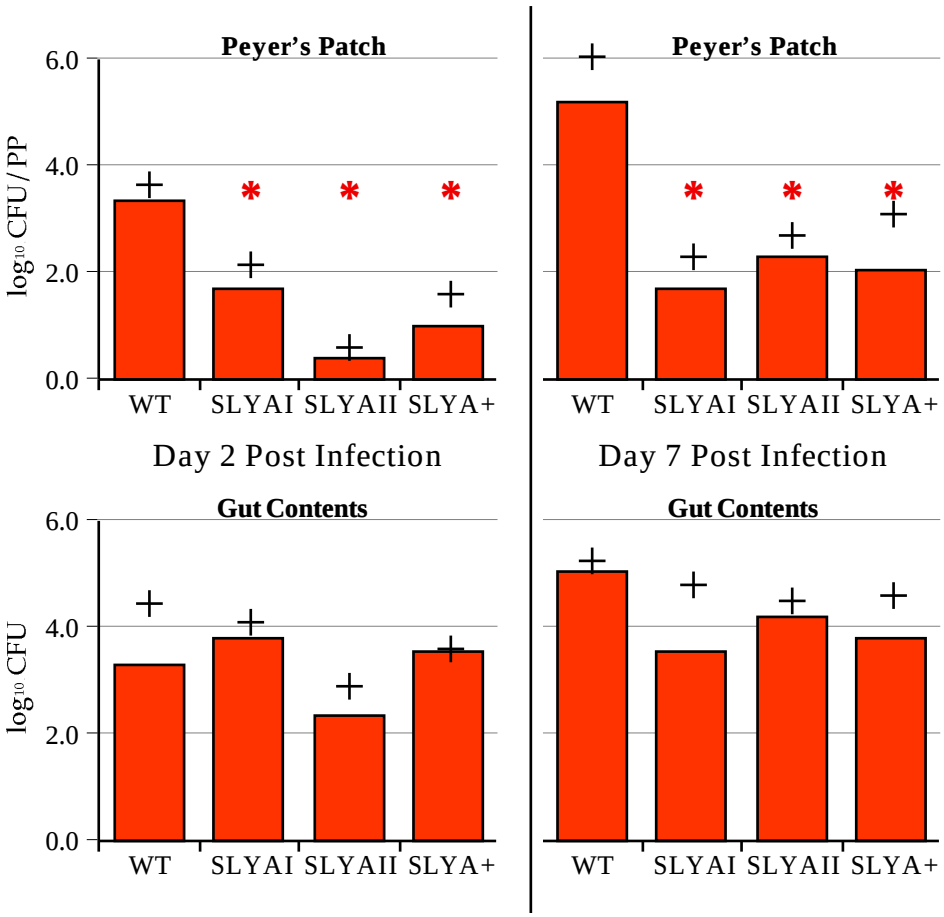

Fig. 3.7. Viable counts of *S. typhimurium* strains found in the lumen of the small intestine and within Peyer's patch tissue, 2 and 7 days after orogastric infection (bars represent the means and the crosses represent one standard deviation of the mean). The * symbol indicates a significant difference between the WT strain and the indicated strain ($P<0.05$).

groups of mice were orogastrically infected with the WT strain *S. typhimurium* 14028s, the two *slyA* insertion mutants, SLYAI and SLYAII, and the SlyA over producing strain *S. typhimurium*/pAL102, respectively. These mice were killed after 2 or 7 days and bacterial numbers were calculated for total small intestine colonisation and Peyer's patch tissue invasion. The ability of the two *slyA* mutants and of *S. typhimurium*/pAL102 to persist within the lumen of the small intestine was not affected after 2 days and only slightly reduced after 7 days when compared to the WT strain (Fig. 3.7), indicating that products needed for survival in, and colonisation of, the lumen of the small intestine are apparently not affected by SlyA. The number of viable bacteria found within Peyer's patch tissue 2 and 7 days after orogastric infection (Fig. 3.7) was, however, significantly reduced

for both *slyA* mutants and the SlyA over producing strain when compared to the WT ($P < 0.05$).

3.2.5. Invasion and Survival in Peyer's Patch Tissue by the *S. typhimurium* Strains

The question therefore arose as to whether the derivative strains had reduced invasion capability, or were unable to survive the onslaught of host defences once invasion into the FAE had occurred. To resolve this question ligated ileal loop tests were performed with an infection time of 90 min. After infection the excised Peyer's patches were treated with gentamicin to kill extracellular bacteria and CFUs were determined from the homogenised tissue to analyse invasion into Peyer's patches. Two controls were used in these experiments: the wild type *S. typhimurium* as a positive control and a mutant strain of *Yersinia enterocolitica* (*inv*$^-$ and cured of the virulence plasmid) as an invasion negative control. The gentamicin minimum bactericidal concentration values for the *Y. enterocolitica* strain and all *S. typhimurium* strains were equivalent. The *Y. enterocolitica* was included to determine "background" bacterial counts. This strain showed negligible invasion (Fig. 3.8) demonstrating that this procedure was useful in determining numbers of bacteria invaded into Peyer's patch tissue. It was found that bacterial numbers in Peyer's patch tissue were similar for all the *S. typhimurium* strains (Fig. 3.8). These results suggest that invasion is not affected by SlyA, and taken together with the previous results (3.2.4.), indicates that

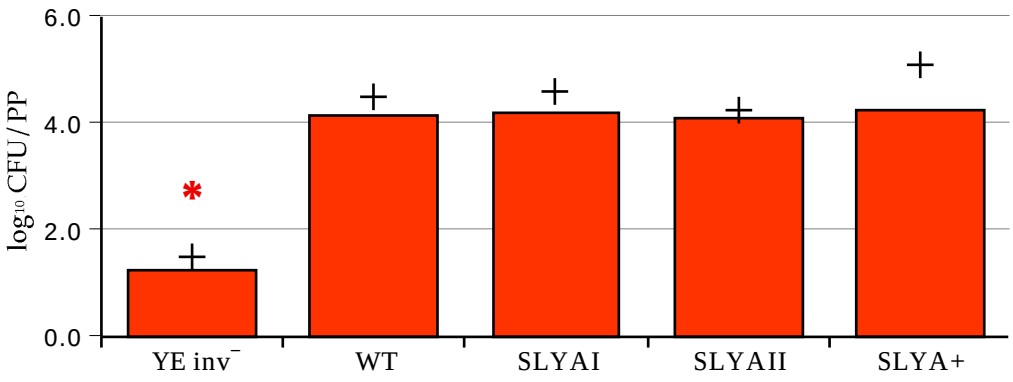

Fig. 3.8. Invasion of Peyer's patch tissue after loop infection (90 min) by *S. typhimurium* strains. YE inv$^-$=*Yersinia enterocolitica* cured of virulence plasmid and containing a Δ*inv* mutation. The * symbol indicates a significant difference between the WT strain and the indicated strain (P<0.05).

survival is, at least in part, affected by SlyA.

3.2.6. Electron Microscopy Analysis of the Infected Peyer's Patch Tissue from Intestinal Loops.

To ascertain tissue pathology and to characterise the stages of invasion and cytotoxicity of the *S. typhimurium* strains, electron microscopy was performed on Peyer's patch tissue at different time points after ligated ileal loop infection. Transmission electron microscopy revealed similar results to Jones *et al.* (1994) during the 180 min of WT *S. typhimurium* infection of the ileal loop. Briefly, induction of ruffling of, and invasion into, M cells by the WT strain was observed after 60 min (Fig. 3.9A); after 120 min the WT was cytotoxic for M cells and disrupted tight junctions causing occasional sloughing of FAE away from the basal lamina (Fig. 3.9B); after 180 min the whole dome area was often completely denuded of enterocytes (Fig. 3.9C). In contrast to these findings, the two *slyA* insertion mutants, SLYAI and SLYAII, and the *S. typhimurium*/pAL102 strain, had significantly altered pathogenic phenotypes. Both *slyA* mutants also caused

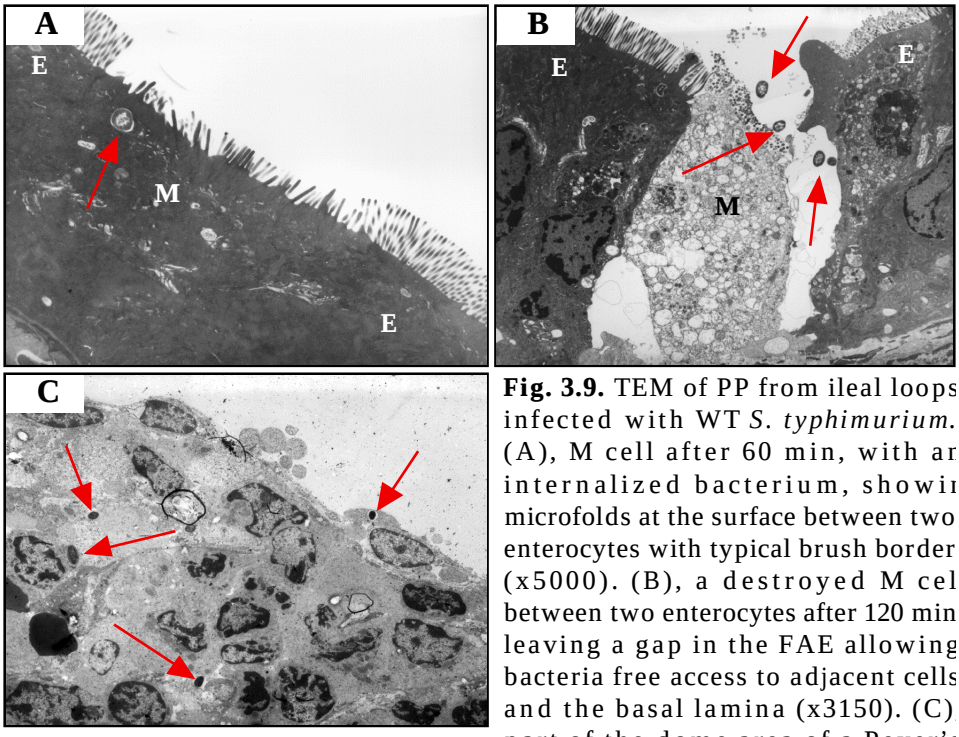

Fig. 3.9. TEM of PP from ileal loops infected with WT *S. typhimurium*. (A), M cell after 60 min, with ar internalized bacterium, showi microfolds at the surface between two enterocytes with typical brush border (x5000). (B), a destroyed M cel between two enterocytes after 120 min leaving a gap in the FAE allowing bacteria free access to adjacent cells and the basal lamina (x3150). (C) part of the dome area of a Peyer's patch after 180 min completely stripped of the FAE, exposing the basa lamina; invaded bacteria can also be seen (x3000). E=enterocyte, M=M cell, arrows=bacteria.

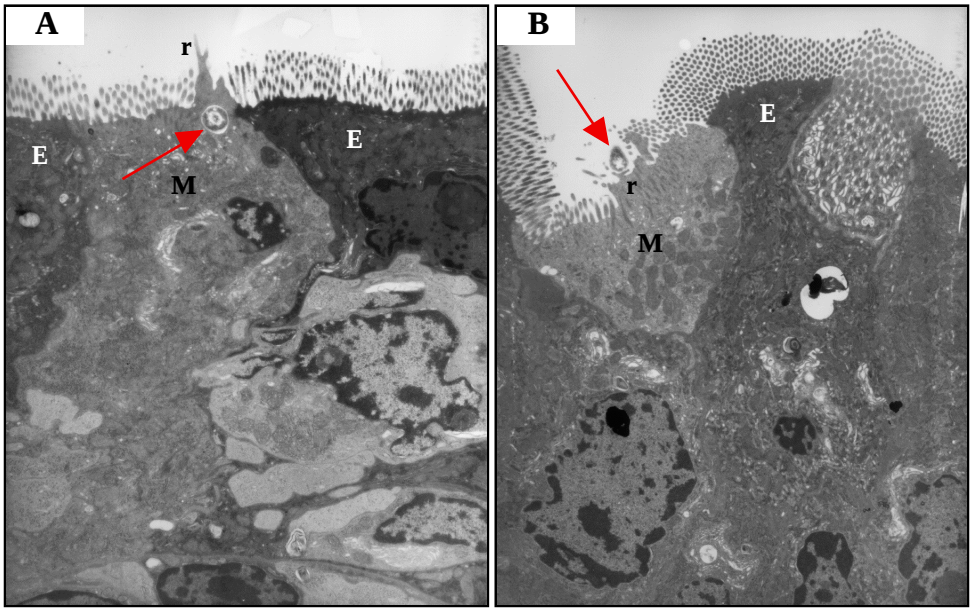

Fig. 3.10. TEM of *S. typhimurium* mutant SLYAII infected PP from ileal loop experiments. (A), ruffled M cell after 60 min with an internalized bacterium (x6000). (B), after 180 min M cell in the process of engulfing a bacterium via ruffling (x6000). E=enterocyte, M=M cell, r=ruffling, arrows=bacteria.

ruffling of, and invaded into, M cells after 60 min (Fig. 3.10A); and after 120 min many M cells were in a state of gross apical membrane rearrangement (ruffling); but after 180 min there were only a few destroyed M cells within the FAE to be observed (Fig. 3.10B). The WT strain carrying multiple copies of *slyA*, *S. typhimurium*/pAL102, induced ruffling of, and invaded into, M cells after 60 min (Fig. 3.11A); after 120 min M cells, and some adjacent enterocytes, were observed to be in the process of dying (Fig. 3.11B); and after 180 min many M cells were infected and dying, and adjacent enterocytes were highly vacuolated, seemingly in the process of dying, but invaded bacteria in these cells were only occasionally seen (Fig. 3.11C). However, at this time point the integrity of the FAE was still intact, and only rare sloughing away of the FAE from the basal lamina was observed.

Scanning electron microscopy (SEM) was used to examine the gross effect of the four bacterial strains on Peyer's patches and to confirm the TEM. The WT was observed to have denuded nearly all enterocytes and M cells from the dome areas after 180 min (Fig. 3.12A) exposing porous underlying tissue (McClugage et al, 1986), whereas the mutant strains, SLYAI and SLYAII, and *S.*

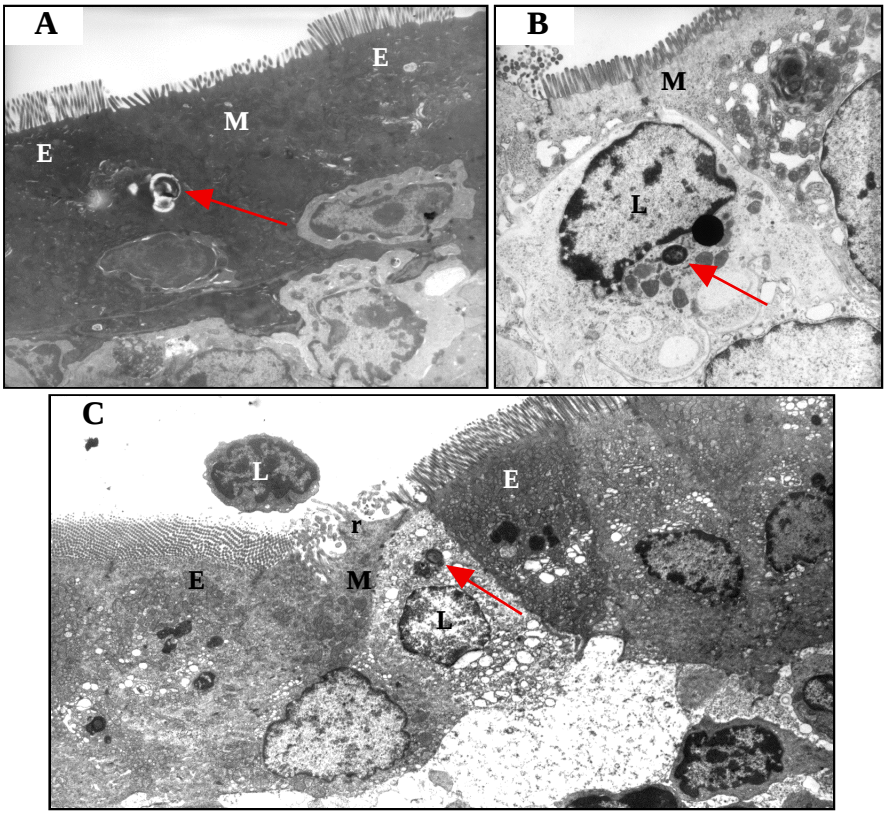

Fig. 3.11. TEM of *S. typhimurium* / pAL102 infected PP from ileal loop experiments. (A), bacterium in M cell after 60 min (x4000). (B), bacterium in lymphoid cell that has pushed into an M cell, after 120 min (x6300). (C), ruffled M cell containing a lymphoid cell which has ingested a bacterium after 180 min; adjacent enterocytes can be seen with an increased number of vacuoles, and a lymphoid cell in the lumen, which presumably has escaped through disrupted FAE elsewhere in the PP (x4000). E=enterocyte, M=M cell, L=lymphoid cell, r=ruffling, arrows=bacteria.

typhimurium / pAL102 had little effect on the integrity of the FAE after the same time (Figs. 3.12B and 3.12C).

To demonstrate statistically significant differences between strains, M cells were counted, and their state of interaction with the different strains of bacteria noted, as determined by TEM. At least 5 sections were examined from each Peyer's patch from at least 5 mice for each bacterial strain and for each loop incubation time. Percentages of M cells affected were calculated for three types of interaction: ruffling (eg Figs. 3.10A and 3.10B), invasion (eg Figs. 3.9A, 3.10A, and 3.11B), and destruction (eg Fig. 3.9B); arithmetic means and standard deviations were then calculated (Table 3.1). M cell ruffling was observed significantly more frequently ($P < 0.05$) after 120 min with the two *slyA* mutants and also after 180 min with the SlyA over producing strain, when compared to the WT. This effect was

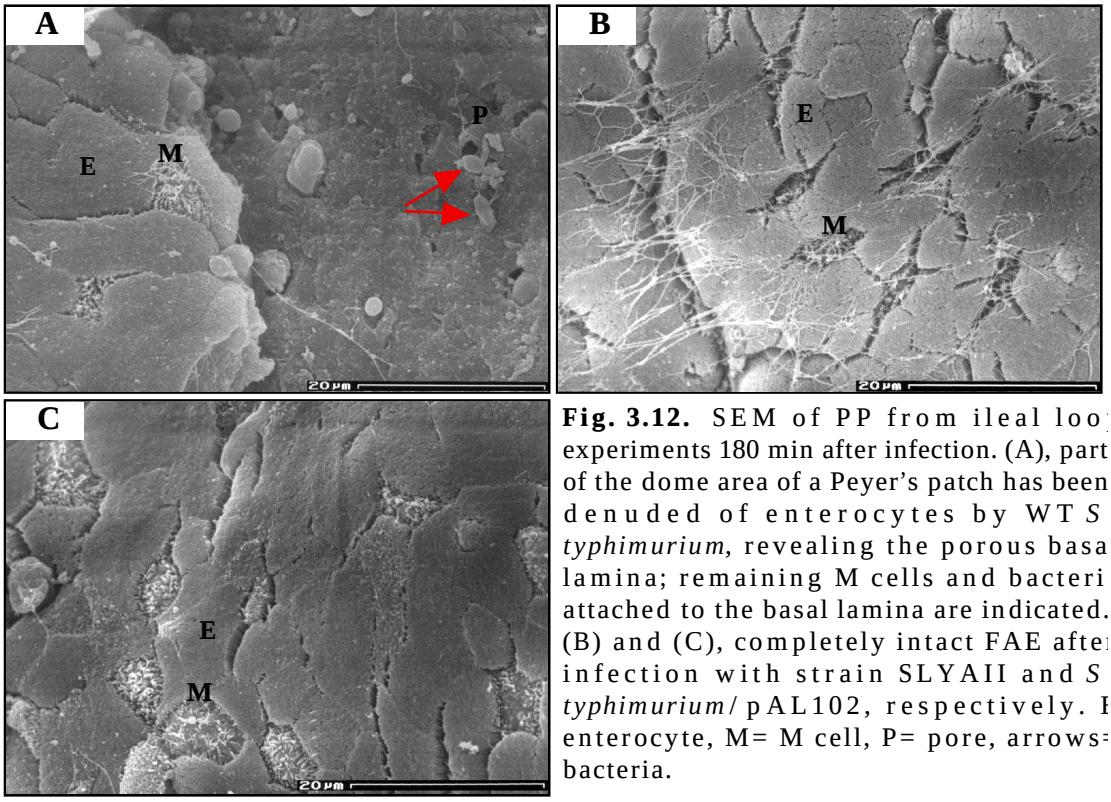

Fig. 3.12. SEM of PP from ileal loo experiments 180 min after infection. (A), part of the dome area of a Peyer's patch has been denuded of enterocytes by WT *S typhimurium*, revealing the porous basa lamina; remaining M cells and bacteri attached to the basal lamina are indicated. (B) and (C), completely intact FAE afte infection with strain SLYAII and *S typhimurium*/pAL102, respectively. E enterocyte, M= M cell, P= pore, arrows= bacteria.

probably due to the WT destroying M cells shortly after internalisation, and hence reducing the available population of M cells, so comparisons with the WT at 180 min have limited value. No significant difference was observed in invasion between the WT strain, and both *slyA* mutants for the entire 180 min, but after

	% M cells affected at different time points [b]:		
	60 min	**120 min**	**180 min**
Ruffling			
WT	28.3±18.1	25.0±19.7	2.4±6.3
SLYAII	30.0±26.2	49.1±16.3 *	61.0±26.9 *
S. typhimurium/pAL102	35.1±6.8	22.0±6.6	22.6±5.5 *
Invasion			
WT	9.5±16.3	9.7±10.1	5.5±10.8
SLYAII	10.3±12.1	7.2±8.3	6.7±9.4
S. typhimurium/pAL102	14.2±1.8	55.5±8.9 *	66.4±14.3 *
Destruction			
WT	13.3±13.6	43.2±28.3	90.7±12.2
SLYAII	6.8±13.6	6.8±7.8 *	18.0±6.5 *
S. typhimurium/pAL102	6.6±5.1	12.6±3.2 *	18.0±4.5 *

Table 3.1. *S. typhimurium* interaction with M cells after loop infection, as determined by transmission electron micoscopy. Values are from one experiment, with each value being calculated from a sample of 5 mice, with an average of 20 M cells counted per mouse. % mean of M cells affected ± SD. Asterisks (*) indicate values that differ from the WT at a $P < 0.05$. Results are for SLYAII only, but comparable results were obtained with SLYAI. Destruction was typically observed as M cells with large numbers of vacuoles, disrupted tight junctions and cell contents spewing into the lumen of the small intestine.

120 min and 180 min the SlyA over producing strain was seen inside living M cells at a much higher frequency than the normal WT strain ($P < 0.05$). Many of these M cells infected with the SlyA over producing strain were highly vacuolated and seemingly in the process of dying, although the integrity of the FAE was still intact. The most striking of all the differences was the effect of the WT in destroying M cells when compared to the *slyA* mutants and the SlyA over producing strain: after 60 min no significant difference could be observed, but after 120 min and 180 min dissimilarity was obvious as the WT was much more cytotoxic to M cells than the *slyA* mutants and the SlyA over producing strain ($P < 0.05$). No invasion was seen via the apical side of normal enterocytes by any of

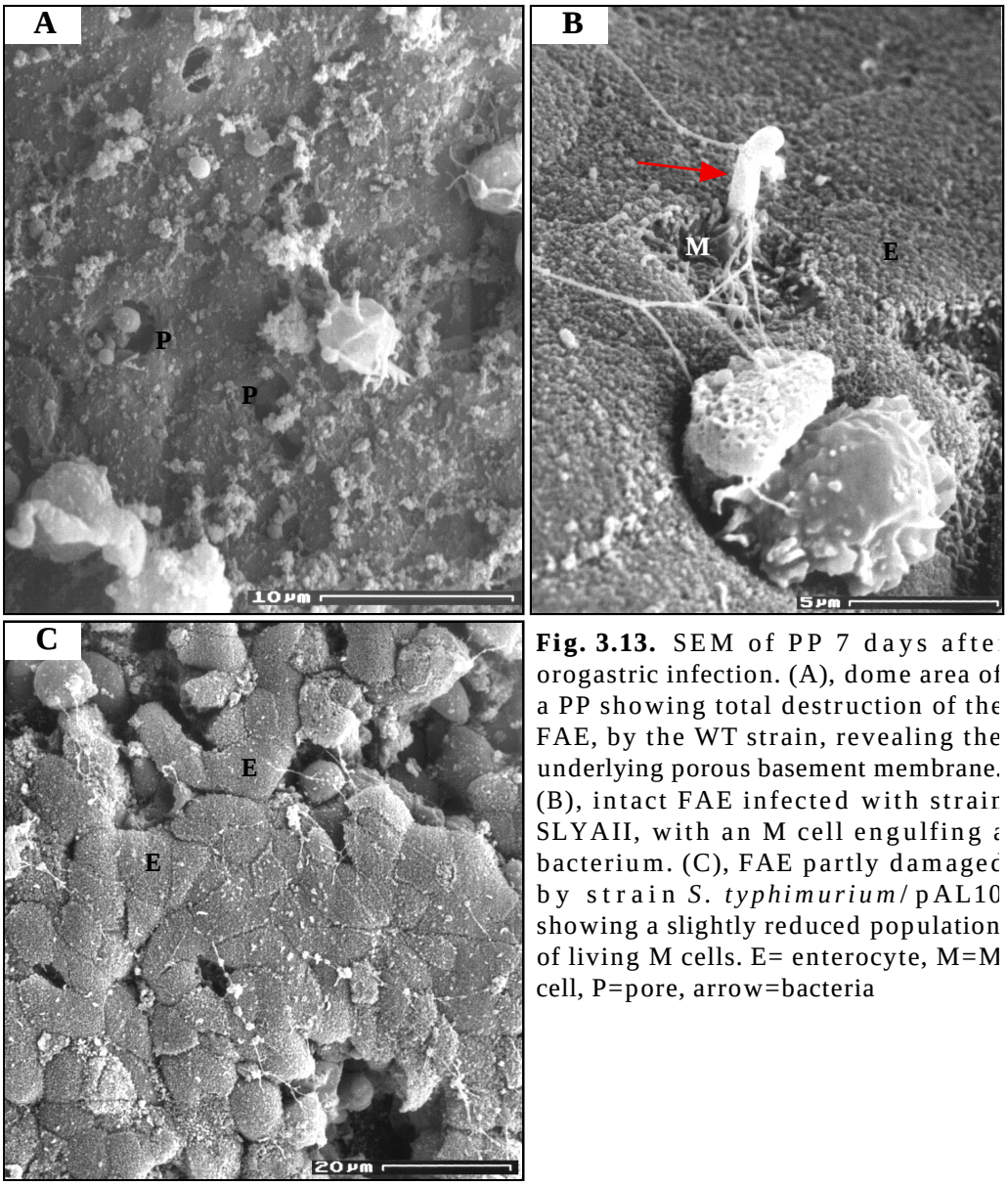

Fig. 3.13. SEM of PP 7 days afte orogastric infection. (A), dome area of a PP showing total destruction of the FAE, by the WT strain, revealing the underlying porous basement membrane. (B), intact FAE infected with strain SLYAII, with an M cell engulfing a bacterium. (C), FAE partly damaged by strain *S. typhimurium*/pAL10 showing a slightly reduced population of living M cells. E= enterocyte, M=M cell, P=pore, arrow=bacteria

the strains.

3.2.7. Electron microscopy analysis of the infected Peyer's patch tissue after orogastric infection.

As *S. typhimurium*/pAL102 was seen to induce stress in M cells and neighbouring enterocytes after 180 min in the loop model, it was therefore important to determine the fate of these cells at later time points in the infection. This was impossible using the loop model as it is problematic to keep small animals, such as mice, under anaesthetic for long periods. Consequently, Peyer's patch tissue from mice was examined by SEM 7 days after orogastric infection of 10^7 CFU. The WT strain induced extensive damage to Peyer's patches (Fig. 3.13A), but strains SLYAI and SLYAII induced no visible pathology of the dome areas or surrounding villi (Fig. 3.13B). The SlyA over expressing strain, *S. typhimurium*/pAL102, was observed to have destroyed some cells of the FAE (Fig. 3.13C), and the destroyed cells were probably M cells, as the countable population of M cells was slightly below that of normal FAE. However, there was no large scale pathology observed.

3.3. Interaction of *L. monocytogenes* with the Murine Host

The primary objective of the following experiments was to determine the route of entry that *Listeria monocytogenes* takes after arriving in the gastrointestinal tract. Some workers have already postulated that *L. monocytogenes* enters via M cells (Dramsi et al, 1996) just like *Shigella flexneri* (Perdomo et al, 1994) and *Salmonella typhimurium* (Jones et al, 1994, Clark et al, 1994), however direct evidence for this is lacking, and at most very circumspect. Therefore, it was undertaken to establish if *L. monocytogenes* has any specificity for particular epithelial cell types, especially M cells.

3.3.1. Invasion of the Small Intestine by *L. monocytogenes* and Subsequent Dissemination to Deeper Organs

One of the problems with comparing the findings of others is the myriad of *L. monocytogenes* wild type strains and mouse types used in the different listeriosis models. Therefore, to determine if the results reported by other groups are consistent with the listeriosis model established here, ie *L. monocytogenes* EGD in BALB/c mice, the aforementioned mouse strain was orogastrically infected with $1.0x10^9$ - $2.0x10^9$ CFU *L. monocytogenes* and the infection was followed over a period of 7 days, assessing the bacterial load in different tissue types. The bacterial loads of livers, spleens, Peyer's patches and equivalent sized pieces of non-Peyer's patch small intestine (Fig. 3.14.) all showed a steady rise until day 3-5, whereupon the mice recovered and cleared the *L. monocytogenes.* Day 5 seems to be the the decisive day which determines the fate of the murine host- survival and

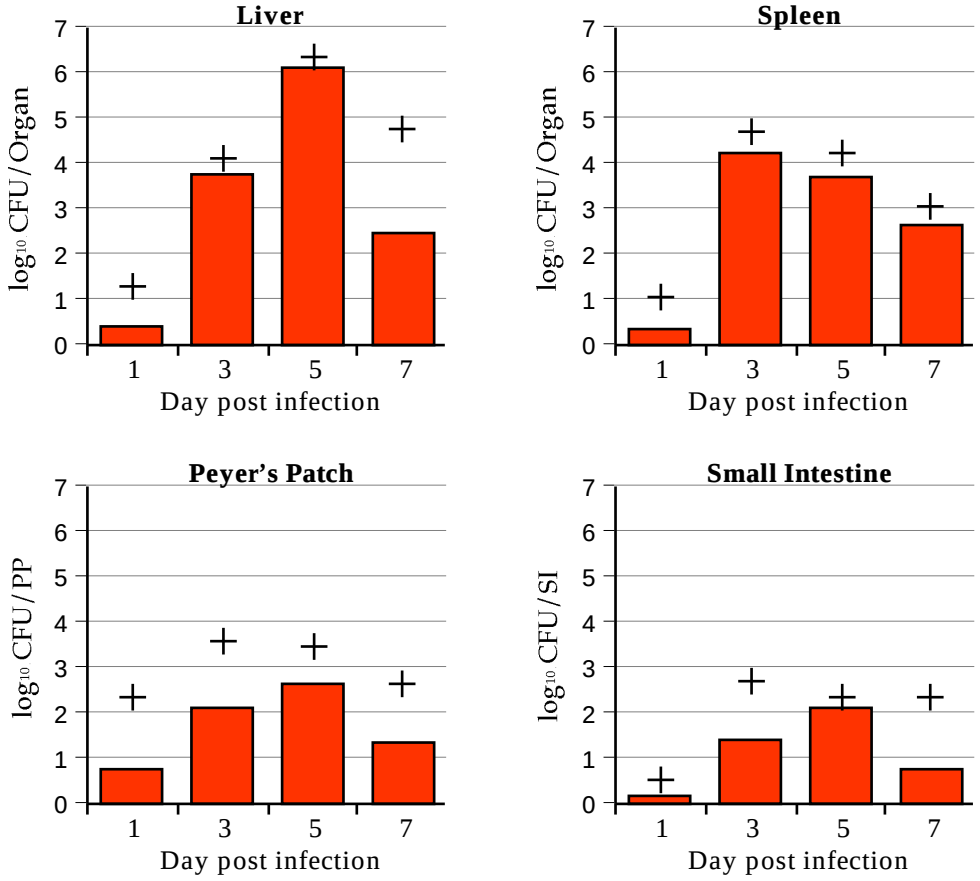

Fig. 3.14. Viable counts of *L. monocytogenes* WT found in different tissues after orogastric infection of mice. Each mouse received ~10^9 CFU which produced a reproducible infection. A consistently higher number of bacteria were found in Peyer's patches, when compared to non-Peyer's patch intestinal tissue.

complete recovery or death. With the dose used here, very few mice died from listeriosis. Also observed was a consistently higher number of bacteria found in Peyer's patches compared with small intestine of approximately 1 log, although no statistical difference was discerned. These results are similar to the findings of MacDonald & Carter (1980).

3.3.2. Translocation of *L. monocytogenes* from the intestinal lumen to the blood and deeper organs

It is clear from the above infection kinetic that *L. monocytogenes* was able to reach deeper organs. However it was not obvious whether the bacteria reached the liver and spleen in large numbers and were then quickly killed, or if only small numbers of bacteria reached these organs which were effective in resisting the host defences. Therefore, ileal loop infections were performed on mice, inoculating the loops with ~10^9 CFU of *L. monocytogenes* or *L. innocua*, and using *Bacillus subtilis* as a negative control. Each loop contained one Peyer's patch. The abdominal cavity was bathed in PBS containing 100 µg / ml gentamicin during the loop procedure to reduce the chance of contaminating the liver and spleen from leakage of the injected bacteria, and the livers and spleens were further incubated for 1 h after removal in BHI containing 100 µg / ml gentamicin. Blood was also taken via heart puncture as another way of obtaining a sterile

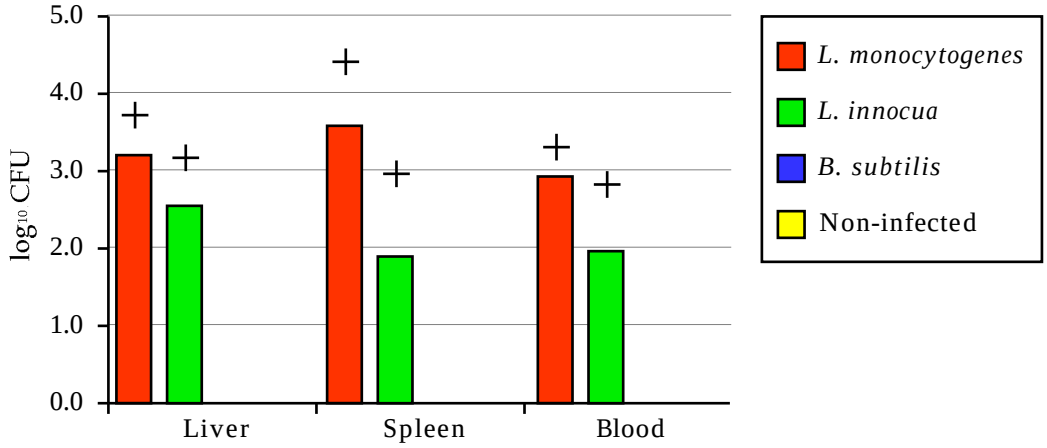

Fig. 3.15. Graph showing numbers viable of bacteria reaching the liver, spleen and blood 30 min after ileal loop infection with different organisms- in contrast to the two *Listeria* spp., *B. subtilis* showed no intestinal translocation. Averages and standard deviations of $\log_{10}$ CFU are shown per organ (livers and spleens) and per ml (blood).

sample, and to determine if arrival of bacteria in the liver and spleen was via the blood. Amazingly, large numbers of bacteria were seen in the livers and blood of mice 30 min after the loops were inoculated (see Fig. 3.15). Furthermore, *L. innocua* was also found in significant numbers showing that invasion was independent of the genes exclusively present in *L. monocytogenes.* Moreover, when loops were inoculated with *Bacillus subtilis* no bacteria were found in the liver or in the blood, indicating that *Listeria* invasion was not due to passive diffusion, nor through artifacts induced by the ileal loop procedure. These findings support those previously reported by Pron et al (1998) for *L. monocytogenes* and *L. innocua,* albeit in another animal model, and demonstrate that *L. monocytogenes,* and even *L. innocua,* can arrive in the deeper organs quickly via the blood after an intestinal infection.

3.3.3. Microscopical Analysis of *L. monocytogenes* Interaction with Intestinal Tissue

Given the preference of *L. monocytogenes* for Peyer's patch tissue after orogastric inoculation, one could expect that either invasion was more efficient in this location, or that survival was better. To answer this question SEM analysis of Peyer's patches and villus tissue was performed after orogastric infection of mice. However, only very rarely were rod shaped bacteria observed, characteristic of *L. monocytogenes,* attaching to epithelial cells (Fig. 3.16A). By far the predominant observation was tissue devoid of *L. monocytogenes* shaped bacteria. Segmented

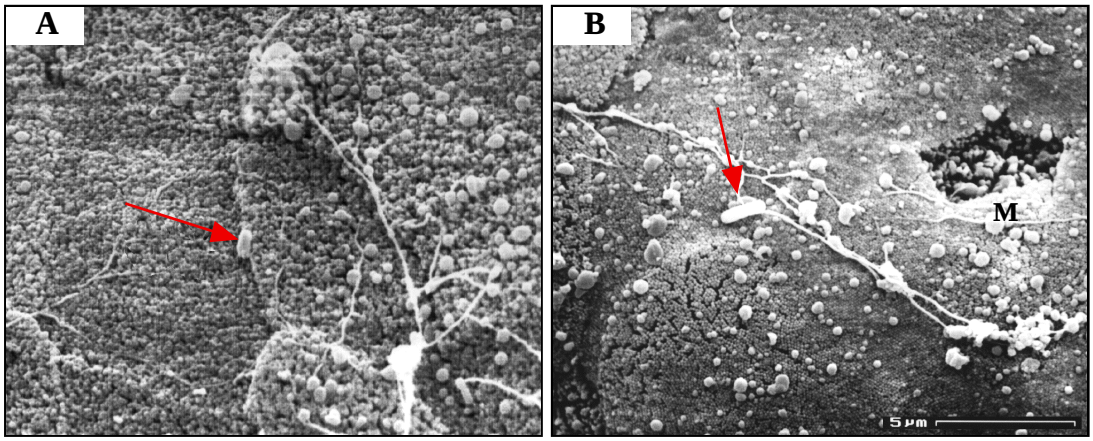

Fig. 3.16. SEM of FAE after orogastric (A) or ileal loop (B) infection with *L. monocytogenes.* After washing of the tissue bacteria were sparsley distributed over the FAE with no apparent preference for M cells. M=M cell, arrows=bacteria.

filamentous bacteria (SFB) were often seen colonising the FAE (Fig. 3.2). SFBs are part of the normal bacterial flora already reported for rodents and other animal species (Klaasen et al, 1992).

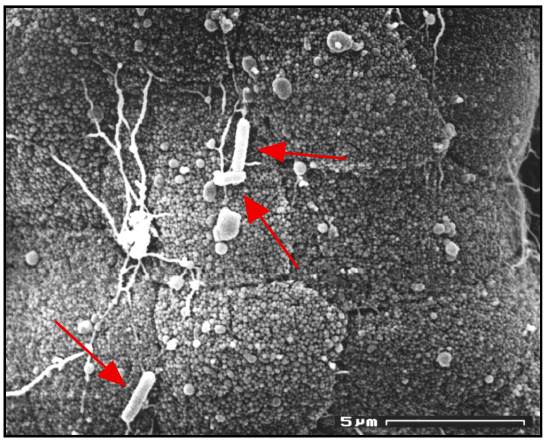

Fig. 3.17. SEM of villus epithelium after ileal loop infection with *L. monocytogenes*. Bacteria were seen attached to villus epithelium just as frequently as bacteria attached to FAE. Arrows=bacteria.

Because it was difficult to see anything definitive after orogastric infection, the ligated ileal loop model was used to increase the chance of observing the events that occur during *L. monocytogenes* invasion of intestinal epithelium. In the ligated ileal loop test a very large inoculum of *L. monocytogenes*, (~10^9 per loop) was used which was similar to that used by Pron et al (1998) using a rat model, and by Jensen et al (1998) using a murine model. Despite the high dose, very little attachment to, or invasion of, the epithelium was seen over a 120 min time period, although significantly more so than tissue analysed from orogastrically infected mice. Rod shaped bacteria attached to columnar epithelial cells of the upper villi were observed (Fig. 3.17), as also seen by Rácz et al (1972), and to the epithelial cells and M cells of the FAE (Fig. 3.16B). These rod shaped bacteria were not seen in non-infected tissue (see Fig. 3.1). Very occasionally, M cells had numerous bacteria associated with the apical membrane causing significant membrane alterations (Fig. 3.18), but no such membrane alteration of columnar epithelial cells was observed. Additionally, no bacteria were seen within the crypt areas between villi.

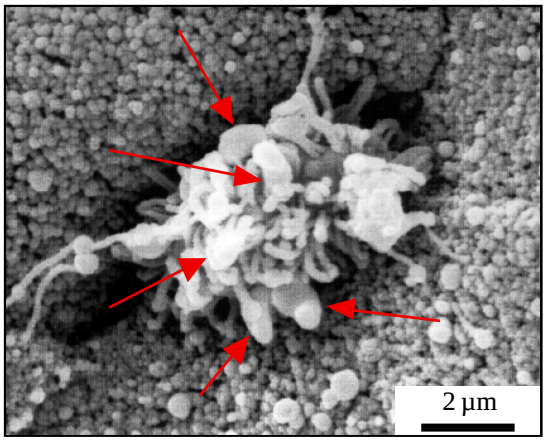

Fig. 3.18. SEM of an M cell apical membrane full with bacteria after ileal loop infection with *L. monocytogenes*. Arrows=bacteria.

Due to the low incidence of attachment of *L. monocytogenes* to epithelial cells seen, even after ileal loop tests, confocal microscopy was used to further study the

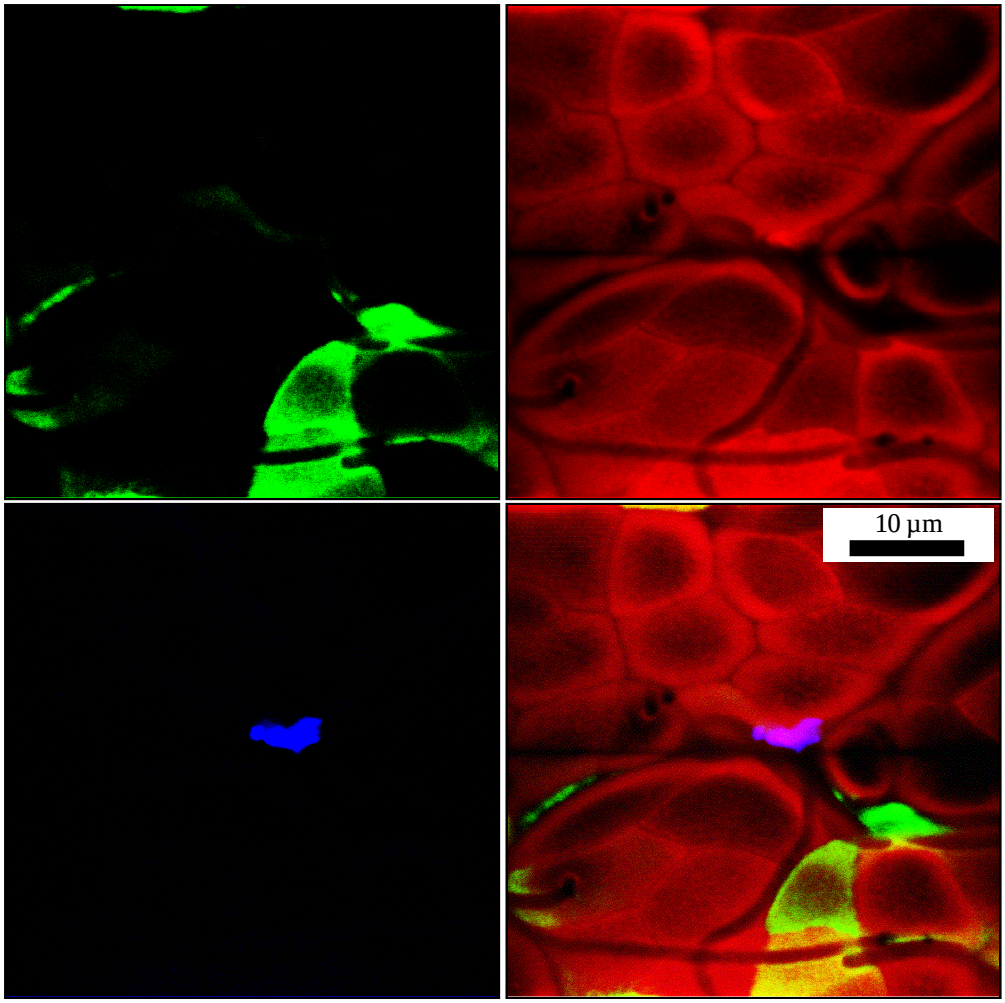

Fig. 3.19. SCLM image of part of a dome area of a murine Peyer's patch, after ileal loop infection with *L. monocytogenes.* Typically, only few bacteria were seen attached to the FAE, showing no preference for M cells The upper left image is stained with FITC-conjugated UEA-1 which is a marker of murine M cells, the upper right image is stained with TRITC-conjugated phalloidin revealing the actin cytoskeleton of cells, the lower left image is stained with a polyclonal anti-*L. monocytogenes* antibody, the lower right image is an overlay.

interaction of *L. monocytogenes* with the FAE of Peyer's patches. Using the lectin from *Ulex europaeus* (TRITC labelled) which specifically binds to the apical surface of murine M cells (Clark et al, 1993), FITC labelled Phalloidin (binds to the actin cytoskeleton which therefore labels all eukaryotic cells) and rabbit derived polyclonal antibodies recognising *L. monocytogenes* (kindly provided by Guido Dietrich, Würzburg University, Germany), it was possible to analyse whether *L. monocytogenes* attached to and / or invaded M cells or non-M cells of the FAE. The findings were very similar to the SEM findings, namely that random distribution of *L. monocytogenes* was seen, and the bacteria showed no preference

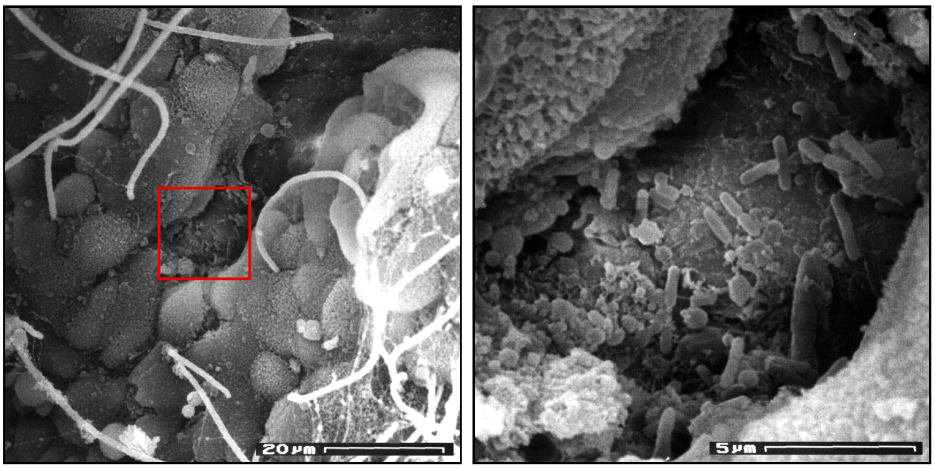

Fig. 3.20. SEM of FAE after loop infection with *L. monocytogenes.* Very occaisionally small areas of damage could be observed within the FAE, where numerous bacteria were seen attached to the revealed basal lamina. This was never seen in villus epithelium. Also, segmented filamentous bacteria can be observed in these SEMs. The red square in the left image indicates the enlarged area shown on the right.

for M cells.

Very infrequently, small areas of the dome areas devoid of FAE were observed (Fig. 3.20). It was not clear whether these areas of damage were induced by the bacteria or if they were present before the infection. These areas of damage were not observed in our non-infected control mice, but it is important to note that the number of control mice used was significantly smaller than the number of infected mice analysed. Nevertheless, within these “holes” numerous rod shaped bacteria were visible (Fig. 3.20) indicating very efficient attachment of *L. monocytogenes* to the basal membrane. No listeria like bacteria were observed adhering to the FAE surrounding these “holes”.

3.3.4. Infection of M cells Grown in Culture by *L. monocytogenes*

The recently reported method of inducing Caco-2 cells of human origin into M cell like cells in vitro (Kernéis et al, 1997) was used to study the behaviour of *L. monocytogenes* in attachment to, and invasion of, a human like FAE. Using a FITC labelled antibody recognising the brush border enzyme sucrase-isomaltase (this enzyme is down regulated in M cells), TRITC labelled Phalloidin and a polyclonal antibody against *L. monocytogenes* the distribution of bacteria over the monolayer could be visualised using confocal microscopy. After numerous

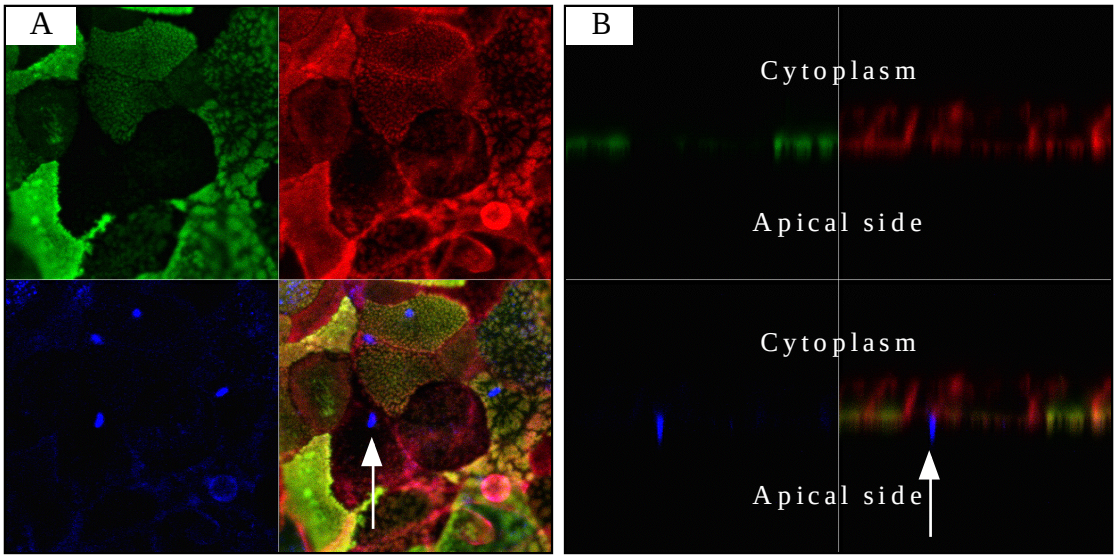

Fig. 3.21. Confocal images of a Caco-2 monolayer with induced M cells infected with *L. monocytogenes*. Enterocytes are stained with FITC-labelled sucrase iso-maltase-antibodies (upper left of A and B)- M cells are not detected with this antibody, the actin cytoskeleton is TRITC-stained (upper right of A and B), and the bacteria are seen as blue (lower left of A and B); the lower right part of A and B is an overlay. Image A shows random distribution of the bacteria on enterocytes and M cells (FITC-negative cells); image B shows an "xz" section of the indicated portion (arrow) of the same monolayer demonstrating M cell invasion.

infections the same pattern was always observed: random distribution and invasion of bacteria over the monolayer (Fig. 3.21), with bacteria attaching to, and invading, enterocytes and M cells (Fig. 3.21). However, no specific targeting of M cells by the bacteria was detected. Analysis of infected monolayers by TEM showed an identical picture of attachment and invasion (Fig. 3.22). Infection o

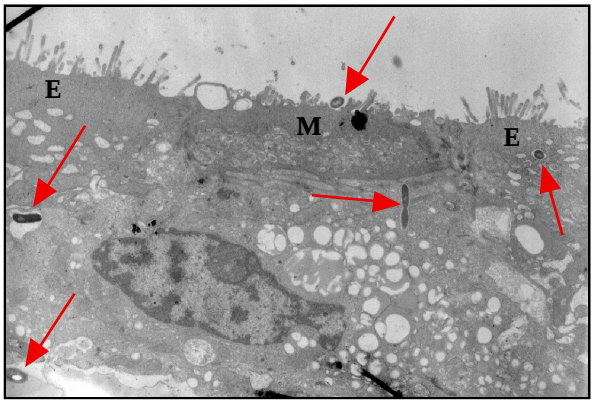

Fig. 3.22. TEM of a Caco-2 monolayer with induced M cells infected with *L. monocytogenes*. Bacteria can be seen, some in the process of dividing, in both enterocytic cells and induced M cells. E=enterocyte, M=M ce arrows=bacteria

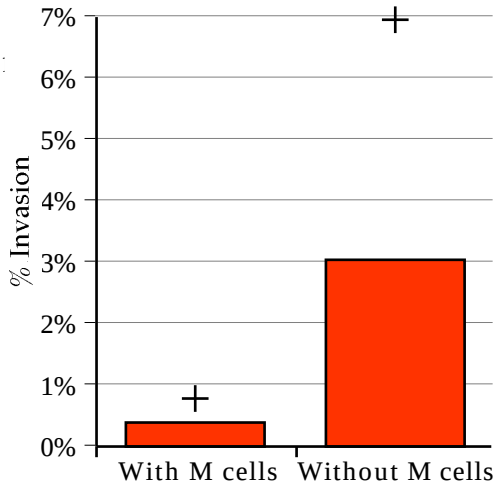

Fig. 3.23. *L. monocytogenes* invasion o Caco-2 monolayers containing and nc containing M cells (MOI=100). Although a variation was always observed, n statistical difference could be determined due to large standard deviations.

monolayers that were not cocultured with lymphocytes also demonstrated attachment and invasion of the apical side by *L. monocytogenes* in a similar pattern and quantity as infected cells cocultured with lymphocytes. When standard gentamicin invasion assays were performed with monolayers containing M cells (cocultured with murine Peyer's patch lymphocytes), and without M cells (no lymphocytes), an increase in the number of invaded bacteria in the monolayers without M cells was seen, although no statistical difference could be detected because of the very large variations within each experiment (Fig. 3.23). Together, these results support the animal work likewise indicating *L. monocytogenes* has no preference for M cells.

3.3.5. InlC of *L. monocytogenes* and its Effect on Virulence

InlC is a recently reported (Engelbrecht et al, 1996) virulence factor of *L. monocytogenes.* However, the function of InlC is, as yet, unknown. Therefore, it was undertaken to go some way in establishing the role of InlC using the mouse model of listeriosis. C57/BL6 mice were used, which are more resistant to *L. monocytogenes* infection, to obtain comparable results with the original data reported in Engelbrecht et al (1996).

3.3.5.1. Infection Kinetics of WT and Δ*inlC L. monocytogenes*

Given the significant increase in the LD_{50} of Δ*inl*C (Engelbrecht et al, 1996), and data indicating that after orogastric infection lower numbers of the Δ*inl*C mutant were present in livers of mice (unpublished results, courtesy of Jürgen Hess), C57/BL6 mice were intravenously infected to bypass the gut stage of listeriosis and hence to determine if the survival in deeper tissues was influenced by InlC. After day 1 post infection a small but, significant difference in the numbers of bacteria in the livers was seen, whereas no difference was seen in the spleens (Fig. 3.24). After 5 days, however, there was a difference of more than two logs between the WT and the Δ*inl*C mutant in the livers of infected mice, and approximately 1.5 logs in the spleens. After 7 days, bacteria were in the process of being cleared and no significant differences were observed.

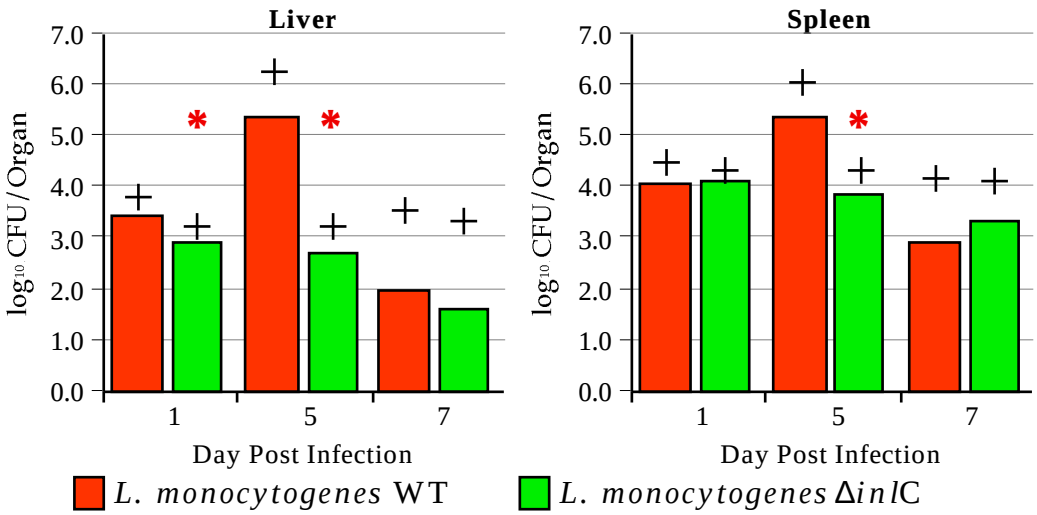

Fig. 3.24. Viable counts of bacteria in livers and spleens of mice intra-venously infected with either *L. monocytogenes* WT or *L. monocytogenes* Δ*inl*C. Asterisks (*) indicate statistically significant differences between the WT and Δ*inl*C mutant.

These data show that the Δ*inl*C mutant is less able to survive or replicate in the systemic organs.

3.3.5.2. Histological Analysis of Livers and Spleens After Infection with WT and Δ*inlC L. monocytogenes*

Given the virulence defect detected in the murine listeriosis model, livers and spleens from iv infected mice were histologically analysed to obtain evidence for a function of InlC. Histological examination showed three distinctive differences between the WT and the Δ*inl*C strains: i) the abscesses induced by the WT were larger than those induced by the Δ*inl*C mutant (Fig. 3.25A & B); ii) the WT strain induced fewer abscesses in livers than the Δ*inl*C mutant (Fig. 3.25 C & D); and iii) later in the infection, livers of mice infected with the WT had noticeably less lymphocyte infiltration than mice infected with Δ*inl*C (Fig. 3.25 E & F).

The fewer abscesses and less lymphocyte infiltration induced by the WT indicate that the Δ*inl*C strain induces a quicker and more effective immune response. The larger foci seen induced by the WT indicates that the WT can spread further before being detected by the immune system. This suggests that InlC may play a crucial role in preventing an effective immune response, perhaps by locally suppressing the immune system or by ‘hiding’ from the immune system.

However, these observations could also indicate a spreading defect.

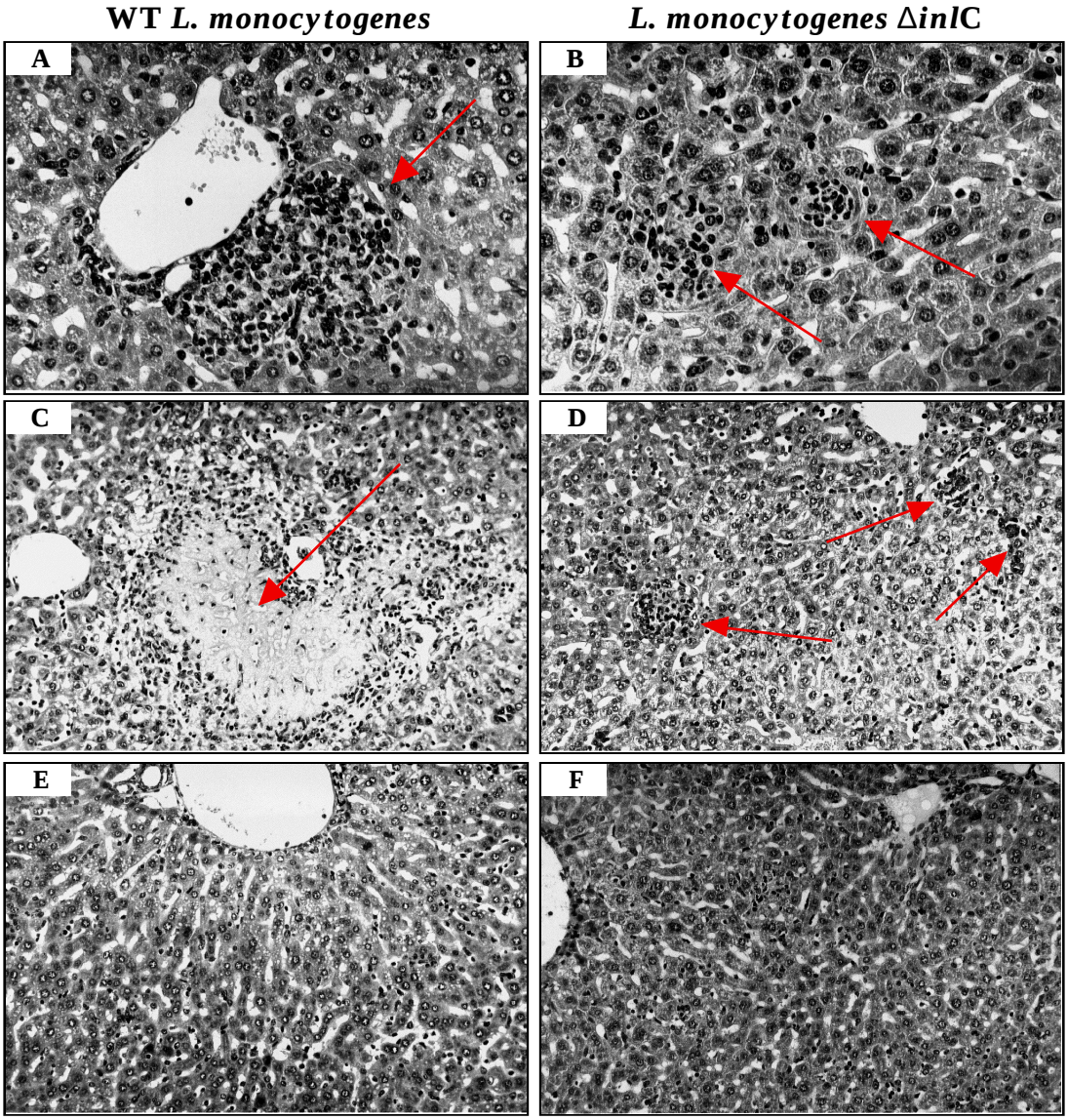

Fig. 3.25. H/E stained parafin sections of livers from mice infected intra-venously with either WT (A, C and E) or Δ*inl*C (B, D and F) *L. monocytogenes*. *L. monocytogenes* WT consistently induced larger (A vs B), but fewer abscesses (C vs D), and less lymphocyte infiltration later in the infection (E vs F) than the Δ*inlC* mutant. The small, darkly stained cells are lymphocytes. Arrows mark the abscesses. Magnification: A and B, x40; C,D,E, and F, x20. Embedding, sectioning and staining kindly performed by the Pathologisches Institut, Universität Würzburg.